Topical Review

Mechanisms underlying the temporal precision of sound coding at the inner hair cell ribbon synapse

Tobias Moser, Andreas Neef and Darina Khimich

InnerEarLab, Department of Otolaryngology, Göttingen University Medical School, Center for Molecular Physiology of the Brain, Bernstein Center for Computational Neuroscience, Göttingen, Robert-Koch-Strasse 40, 37075 Göttingen, Germany

Our auditory system is capable of perceiving the azimuthal location of a low frequency sound source with a precision of a few degrees. This requires the auditory system to detect time differences in sound arrival between the two ears down to tens of microseconds. The detection of these interaural time differences relies on network computation by auditory brainstem neurons sharpening the temporal precision of the afferent signals. Nevertheless, the system requires the hair cell synapse to encode sound with the highest possible temporal acuity. In mammals, each auditory nerve fibre receives input from only one inner hair cell (IHC) synapse. Hence, this single synapse determines the temporal precision of the fibre. As if this was not enough of a challenge, the auditory system is also capable of maintaining such high temporal fidelity with acoustic signals that vary greatly in their intensity. Recent research has started to uncover the cellular basis of sound coding. Functional and structural descriptions of synaptic vesicle pools and estimates for the number of Ca^{2+} channels at the ribbon synapse have been obtained, as have insights into how the receptor potential couples to the release of synaptic vesicles. Here, we review current concepts about the mechanisms that control the timing of transmitter release in inner hair cells of the cochlea.

(Received 6 June 2006; accepted after revision 7 August 2006; first published online 10 August 2006)
Corresponding author T. Moser: Department of Otolaryngology, Göttingen University Medical School, Robert-Koch-Strasse 40, 37075 Göttingen, Germany. Email: tmoser@gwdg.de

Introduction

Hearing relies on faithful synaptic transmission at the ribbon synapse of the auditory hair cell (Fuchs, 2005; Nouvian *et al.* 2006). Figure 1*A* shows a typical inner hair cell with afferent synapses. A well-known phenomenon highlighting the synapse's capability to code temporal fine structure is the phase locking of the auditory nerve fibre's spiking with tonal stimuli up to the low kilohertz range (Kiang *et al.* 1965; Rose *et al.* 1967; Johnson, 1980; Palmer & Russell, 1986). As illustrated in Fig. 1*B* fibres spike preferentially at a certain phase of the stimulus although not every cycle necessarily triggers a spike. The quality of spike synchronization to the phase of the stimulus is described by the synchronization index. It declines with increasing sound frequency (Fig. 1*C*) and decreasing sound intensity. Even at sound levels too low to elicit a significant increase in auditory nerve firing rate, the discharge patterns of the fibre entrain to the stimulus and cluster at a preferred phase of the stimulus cycle. To appreciate the challenge nature faces in achieving temporal acuity of hearing it is worthwhile to look at the cellular processes involved. The neuronal mechanisms underlying the processing of interaural time differences in the auditory brainstem have been reviewed recently (Grothe & Klump, 2000; Grothe, 2003; Konishi, 2003; McAlpine & Grothe, 2003; McAlpine, 2005).

We will focus on the mechanisms that shape the temporal properties of inner hair cell sound coding. Deflection of the hair cell's stereocilia almost instantaneously increases the open probability of the mechanosensitive transduction channels depolarizing the hair cell (Kennedy *et al.* 2003; Ricci *et al.* 2005). The membrane time constant defining the kinetics of hair cell depolarization is determined by its rather small membrane capacitance (Beutner & Moser, 2001; Brandt *et al.* 2003; Michna *et al.* 2003) and the input resistance. The resting conductance is mostly mediated by transduction channels and slow delayed rectifier K^+ channels (KCNQ4) (Marcotti *et al.* 2003; Oliver *et al.* 2003; Kharkovets *et al.* 2006) and may be as low as 1 nS. At the same time, this high input impedance results in a membrane time constant as long as a millisecond and limits the cell's temporal response. Here temporal acuity is killed to insure maximum sensitivity for the encoding of low intensity sounds.

 DOI: 10.1113/jphysiol.2006.114835

Upon sufficient stimulation, however, large conductance Ca^{2+}-activated K^+ channels (BK) and delayed rectifier K^+ channels (K_V) are activated. This rapidly increases the cell's conductance to several nanosiemens and provides for much faster dynamics of the cell's membrane potential (Kros & Crawford, 1990; Kros *et al.* 1998; Zhang *et al.* 1999; Robertson & Paki, 2002; Thurm *et al.* 2005; Oliver *et al.* 2006). Hence, the membrane time constant is a function of the stimulus strength (Kros & Crawford, 1990; Oliver *et al.* 2006). Because gating of BK channels is very fast the cell achieves a fast temporal response in less than a millisecond after the onset of the stimulus. Accordingly, a slowed dynamics of the hair cell's potential and a reduced temporal precision of sound coding were observed in the mouse knockout of the pore forming α-subunit of the BK channel (Kcnma1) (Oliver *et al.* 2006).

The receptor potential opens L-type voltage-gated calcium channels, which mediate the stimulus secretion coupling in cochlear hair cells (Moser & Beutner, 2000; Platzer *et al.* 2000; Spassova *et al.* 2001; Brandt *et al.* 2003, 2005). These $Ca_V1.3$ L-type channels activate at very negative voltages (Koschak *et al.* 2001; Brandt *et al.* 2005). In fact, they drive transmitter release and the resulting spontaneous auditory nerve fibre activity even in the absence of sound (Sewell, 1984; Robertson & Paki, 2002). Their number, spatial distribution and kinetic properties will be reviewed below. Finally, Ca^{2+} triggered fusion of readily releasable vesicles takes place at the ribbon-type active zones of the hair cells. The released transmitter rapidly activates AMPA receptors (Glowatzki & Fuchs, 2002) residing in the postsynaptic density (Matsubara *et al.* 1996) and depolarizes the peripheral axon of the spiral ganglion neuron to threshold, which then conveys the information to its target neurons in the cochlear nucleus. In the following, we will focus on how Ca^{2+} channels couple to exocytosis of synaptic vesicles and how the large readily releasable vesicle pool of the hair cell ribbon synapse contributes to the temporal acuity of sound coding.

Number, spatial distribution and kinetic properties of inner hair cell Ca^{2+} channels

How many Ca^{2+} channels contribute to stimulus–secretion coupling at the hair cell synapse? Using a non-stationary fluctuation analysis on Ca^{2+} tail currents, Brandt *et al.* (2005) demonstrated that mouse IHCs of the apical cochlear turn contain a total of ~1700 Ca^{2+} channels. This is very similar to the analogously estimated Ca^{2+} channel number in frog saccular hair cells (~1800 channels; Roberts *et al.* 1990). In mammalian IHCs around 90% of these channels are of the $Ca_V1.3$-type (Platzer *et al.* 2000; Brandt *et al.* 2003). Several lines of evidence demonstrate that hair cell Ca^{2+} channels cluster at the ribbon-type active zones (Roberts *et al.* 1990; Issa & Hudspeth, 1994; Tucker & Fettiplace, 1995; Rodriguez-Contreras & Yamoah, 2001; Zenisek *et al.* 2003; Sidi *et al.* 2004; Brandt *et al.* 2005). But it is much less clear how many channels are present in the

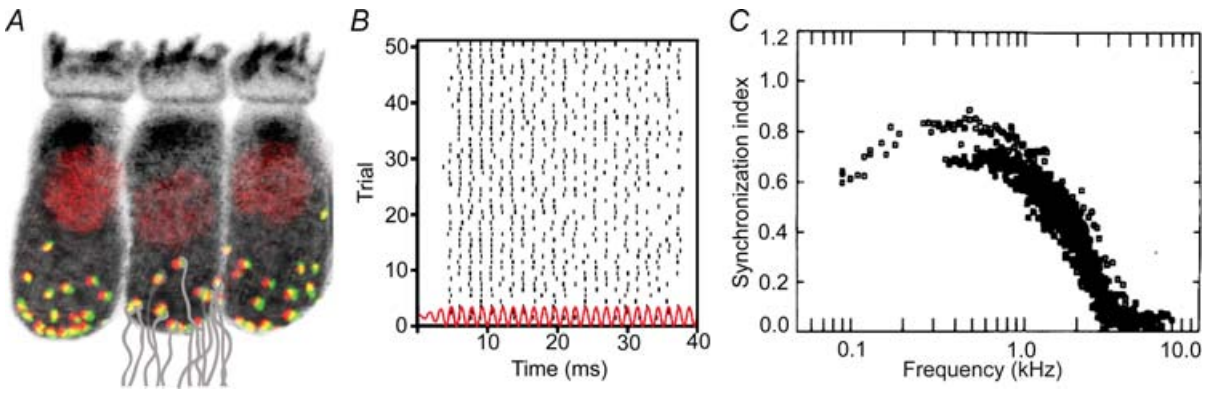

Figure 1. Hair cell afferent synapses in auditory signalling
A, confocal reconstruction of three IHCs within the mouse organ of Corti with immunolabelled IHC bodies (stained for calcium binding protein Calbindin, black), nuclei (stained for CtBP2, red), ribbons (stained for RIBEYE/CtBP2, red) marking the presynaptic active zones and juxtaposed postsynaptic transmitter receptor clusters (GluR2/3 glutamate receptor, green) marking the postsynaptic elements. For illustration we sketched the several postsynaptic fibres (grey) contacting one IHC. *B*, discharge pattern of a chick cochlear afferent fibre recorded *in vivo* in response to 50 repeated presentations of a 676 Hz pure tone. The stimulus frequency is matched to the characteristic frequency of the neuron as determined by a tuning curve. The red line represents the waveform of the acoustic stimulus. Each point signifies the occurrence time of an action potential. Most of the action potentials occur at a preferred phase of the stimulus, a property termed phase-locking (Avissar, Furman, Saunders, Parsons, unpublished data). *C*, phase-locking capability as a function of frequency (quantified by the synchronization index, Rose *et al.* 1967). Data were aquired 20 dB above the mean rate threshold in guinea-pig cochlear nerve (from Palmer & Russell, 1986 with permission from Elsevier).

extrasynaptic membrane. While some authors consider a purely synaptic localization (Schnee *et al.* 2005), a cell-attached patch-clamp study has presented evidence for an appreciable extrasynaptic Ca^{2+} channel density (Rodriguez-Contreras & Yamoah, 2001). Brandt *et al.* (2005) assumed a relatively low channel density: 1 μm^{-2}, as observed in another presynaptic terminal (E. Stanley, personal communication). That led to an estimate of about 80 Ca^{2+} channels at each active zone of mouse IHCs. Only a small fraction of these channels is expected to open upon physiological sound stimulation. Even during maximal *in vitro* stimulation only ~30 channels are activated simultaneously at each active zone. It will be interesting to investigate whether and how the availability of the $Ca_V1.3$ channels for activation is regulated.

The voltage dependence of the Ca^{2+} channel activation shows a $V_{1/2}$ around –25 mV when estimated from whole-cell recordings with extracellular Ca^{2+} concentrations ($[Ca^{2+}]_o$) close to physiological values (Johnson *et al.* 2005; A. Meyer, personal communication). Activation usually starts near the resting potential of the IHCs (–65 mV to –77 mV obtained *in vitro* by patch-clamp (Kros & Crawford, 1990; Brandt *et al.* 2003; Oliver *et al.* 2003), but see (Dallos, 1985; Palmer & Russell, 1986) for more depolarized values up to –45 mV obtained *in vivo* by sharp microelectrode recordings). The time constants for activation of the hair cell Ca^{2+} current vary between a few milliseconds and hundreds of microseconds depending on the stimulus strength (e.g. Zidanic & Fuchs, 1995; Edmonds *et al.* 2004). When considering the temporal constraints imposed on the hair cell synapse to perform faithful sound coding, such 'slow' activation comes as a surprise. Activation kinetics of macroscopic currents has usually been approximated with two exponential terms, indicating the presence of two closed states. In addition to multiple closed states the Ca^{2+} channels of hair cells also display inactivation (Schnee & Ricci, 2003). Therefore, a detailed description of channel gating can only be obtained from single channel recordings. But is this effort necessary to understand sound coding? We would argue for it. As discussed below only one or few Ca^{2+} channels may control the $[Ca^{2+}]_i$ 'seen' by the Ca^{2+} sensor of a nearby docked synaptic vesicle (see next section). Hence, the kinetic properties of single channels might govern exocytosis of readily releasable vesicles.

Unfortunately there is a shortage of single channel data for the $Ca_V1.3$ channel and there are virtually no such data available for mammalian inner hair cells. In a series of papers Rodríguez-Contreras and Yamoah described single Ca^{2+} channel properties in frog saccular hair cells. In these amphibian cells they found L-type Ca^{2+} channels – like the ones that dominate in mammalian IHCs as well as non-L-type Ca^{2+} channels (probably N-type). Here, we focus on their L-type channel data. When we think about the coding of temporal structure, an important property is the delay between stimulus onset and the first channel opening (waiting time). Distributions of waiting times for L-type channels were obtained at near physiological $[Ca^{2+}]_i$ (Rodriguez-Contreras & Yamoah, 2003). They show considerable delay with median waiting times in the range of 5–40 ms (Hess *et al.* 1984; Rodriguez-Contreras & Yamoah, 2003). The interpretation of these values is hampered by the fact that no such distributions have been published for physiological conditions, namely in the absence of gating modifiers and in the presence of low millimolar $[Ca^{2+}]_o$. It remains unclear how coding with high temporal precision can be achieved with such delays. As the total number of Ca^{2+} channels at each hair cell synapse is large, it might be just a matter of statistics that always some channels open within a few hundred microseconds of the stimulus onset. It should be straightforward to find direct answers by single channel recordings in which periodic stimuli mimic the physiological case.

Ca^{2+} nanodomain control of exocytosis by $Ca_V1.3$ channels

How many channels does it take to drive a vesicle's exocytosis? Two extreme scenarios come to mind (Fig. 2). Several Ca^{2+} channels may cooperate to impose a '$[Ca^{2+}]$ microdomain' on the synaptic vesicle's release site at an active zone. Single Ca^{2+} channel gating would average out, such that changes in open channel number or single channel current would each change the $[Ca^{2+}]$ contributing to the microdomain and have indistinguishable effects on exocytosis kinetics (Mintz *et al.* 1995; Wu *et al.* 1999; Augustine, 2001). Such a stimulus–secretion coupling should also reduce the jitter of the Ca^{2+} signal seen by the synaptic vesicle. If, on the other hand, only one or a few Ca^{2+} channels set the $[Ca^{2+}]$ 'seen' by a nearby vesicle, then changes in open channel number or single channel current would each have different effects on exocytosis. Blocking its channel(s) would disable the vesicle's release. Changing the single channel current would change the $[Ca^{2+}]$ seen by the vesicle and consequently release kinetics. Because of the inferred nanometer distance between the channels and 'their' release sites this scenario can been called a Ca^{2+} nanodomain control of exocytosis. In this scenario stochastic single channel gating would substantially contribute to the variance of the synaptic delay.

For interpreting the effects of Ca^{2+} channel manipulation on exocytosis, we need to know how the kinetics of exocytosis depends on the $[Ca^{2+}]$ at the release site. This 'intrinsic' Ca^{2+} dependence of exocytosis was studied using flash photolysis of caged Ca^{2+} (Beutner *et al.* 2001). Small variations among $[Ca^{2+}]$ elevations in the low micromolar range resulted in strikingly different

rates of exocytosis, while the kinetics started to saturate for higher Ca^{2+} concentrations. Similarly, a decline of the exocytic delay was observed with increasing $[Ca^{2+}]$. This Ca^{2+} dependence of exocytosis was modelled as binding of five Ca^{2+} ions to the fusion machinery of a synaptic vesicle followed by a fast fusion reaction ($\sim$1000 s^{-1}). Hence, an intrinsic cooperativity of five is assumed for hair cell exocytosis. The exponent describing the dependence of transmitter release on Ca^{2+} influx is often referred to as the 'apparent' Ca^{2+} cooperativity. This apparent Ca^{2+} cooperativity can approach but not exceed the intrinsic Ca^{2+} cooperativity of exocytosis. The high intrinsic Ca^{2+} cooperativity of hair cell exocytosis should be mirrored by the dependence of exocytosis on Ca^{2+} influx when changing the single channel current (and hence the Ca^{2+} domain amplitude at the site of the vesicle), whatever the topography of channels and docked vesicles might be. On the other hand, finding a much lower power dependency upon changes of the Ca^{2+} channel number would suggest the presence of a Ca^{2+} nanodomain scenario.

In a biophysical study of exocytosis from the readily releasable pool (RRP) of vesicles in mouse IHCs, Brandt *et al.* (2005) demonstrated a high Ca^{2+} cooperativity for changes of the single Ca^{2+} channel current by variation of the extracellular $[Ca^{2+}]$. A supralinear rise of exocytosis with the number of incoming Ca^{2+} ions was observed in the low $[Ca^{2+}]$ range, as expected from the high intrinsic Ca^{2+} cooperativity of hair cell exocytosis.

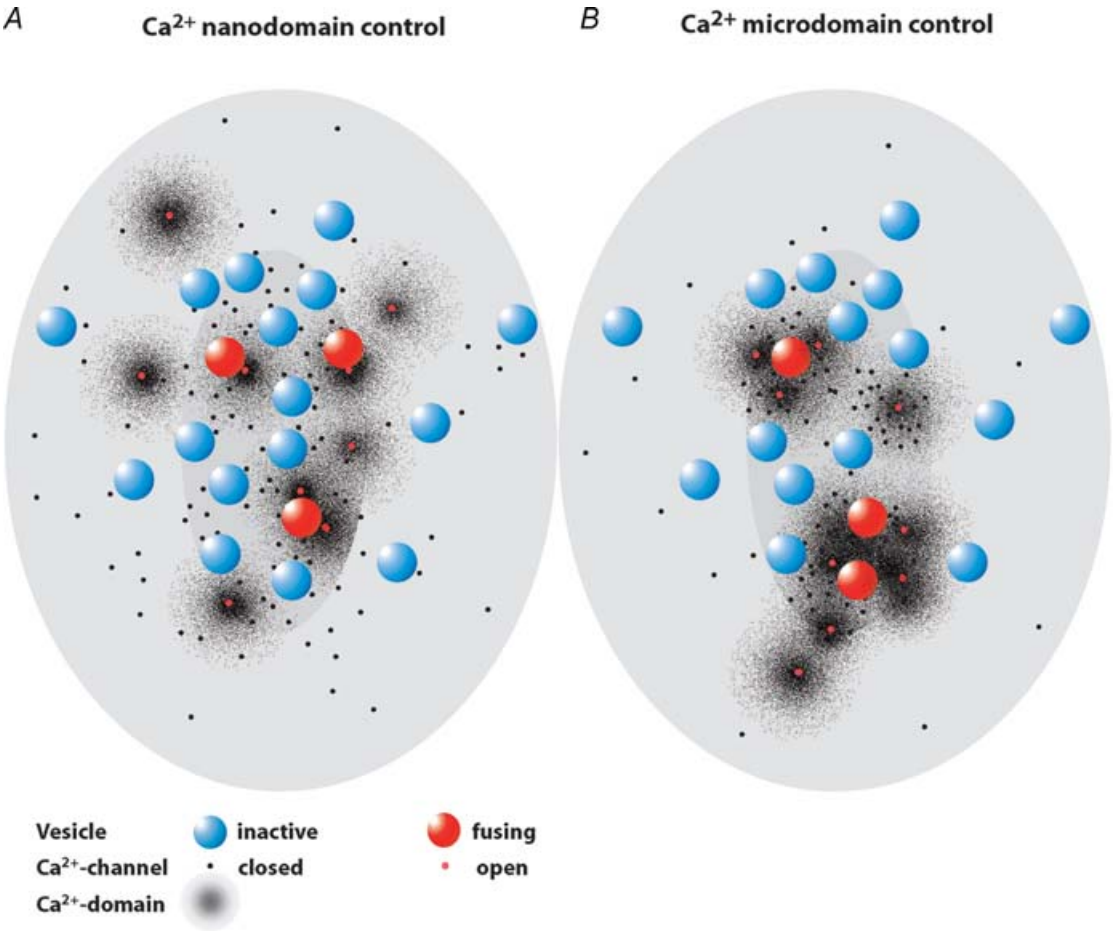

Figure 2. Ca^{2+} nanodomains *versus* Ca^{2+} microdomains
Cartoons sketch the IHC active zone seen from hair cell cytosolic site with the ribbon removed (central ellipse indicates the ribbon's projection) facing the postsynaptic density (outer ellipse). The figure illustrates two different topographies of Ca^{2+} channels (80, black and red spots) and docked vesicles (16, blue and red spheres) that could lead to Ca^{2+} nanodomain (*A*) or Ca^{2+} microdomain (*B*) control depending on further parameters such as Ca^{2+} buffering and Ca^{2+} dependence of exocytosis. *A*, 80 Ca^{2+} channels were scattered at the active zone with a higher density underneath the ribbon and an increased likelihood to be close to a docked vesicle. Synaptic vesicles preferentially dock to the plasma membrane opposite to the postsynaptic density. At the time of observation the depolarization had opened 9 channels (red) forming small Ca^{2+} domains of elevated $[Ca^{2+}]$, some of which drive fusion of 'their' nearby vesicles (red vesicles). *B*, most of the 80 channels are placed in 3 channel clusters, where a number of them cooperate to form larger Ca^{2+} microdomains.

However, exocytosis tended to saturate for larger amounts of Ca^{2+} influx. It is attractive to consider that a further increase of the Ca^{2+} domain around Ca^{2+} channels was not efficient in triggering more exocytosis, because fusion, but not any longer Ca^{2+} binding, was rate limiting. When blocking hair cell Ca^{2+} channels bit by bit by slow application of dihydropyridine (DHP) antagonists they observed a low Ca^{2+} cooperativity of exocytosis. As shown by single channel studies (Hess *et al.* 1984) DHP antagonists do not change the single Ca^{2+} channel current but decrease the channel open probability. Hence, Brandt and colleagues interpreted the antagonistic DHP action as primarily changing the number of open channels. In one set of experiments they combined the change of $[Ca^{2+}]_o$ with application of the DHP antagonist nifedipine at saturating $[Ca^{2+}]_o$ (10 mM). Whereas the increase of Ca^{2+} influx upon changing $[Ca^{2+}]_o$ from ~4–10 mM (change of single channel current) caused very little increase of RRP exocytosis, they found an immediate decline of exocytosis with the reduction of Ca^{2+} influx after reduction of available Ca^{2+} channels by nifedipine.

How then does Ca^{2+} influx elicited by varying sound intensities relate to hair cell exocytosis? The resulting receptor potentials cause opening of different numbers of Ca^{2+} channels and, due to the change of driving force for Ca^{2+}, also change the single channel current. The apparent Ca^{2+} cooperativity of exocytosis observed during changes of the depolarization level was low (Johnson *et al.* 2005; Keen & Hudspeth, 2006). In the case of nanodomain control of exocytosis this finding is expected for the physiological voltage range in which the increase in open channel number dominates over the reduction of single channel current. Evidence for Ca^{2+} nanodomain overlap (Zucker & Fogelson, 1986; Augustine *et al.* 1991) was found for a strong depolarization (Brandt *et al.* 2005), where more exocytosis was elicited than at a weaker depolarization for the same Ca^{2+} current.

The Ca^{2+} nanodomain hypothesis was further supported by the higher potency of the added fast-binding Ca^{2+} chelator BAPTA, when compared to the slow-binding EGTA (Moser & Beutner, 2000). Such a Ca^{2+} nanodomain control of exocytosis would result in a high $[Ca^{2+}]$ at the vesicle's release site, ensuring fast exocytosis following channel activation. This would reduce the time needed for exocytosis of a given vesicle to a rather invariant delay and make the regulation of 'its' Ca^{2+} channel(s) the key parameter also for defining the temporal response of the synapse. Sound evoked receptor potentials of different amplitude would then recruit varying numbers of these functional Ca^{2+} channel–vesicle release site units, but release each vesicle at comparable speed following Ca^{2+} channel opening. This may represent the mechanism behind Furukawa's classical observation that stimulus intensity varies the number of release sites rather than the probability of release for a given synaptic vesicle (Furukawa *et al.* 1978; Furukawa *et al.* 1982; Furukawa & Matsuura 1978).

This brings us back to the $Ca_V1.3$ channel gating and the lack of single channel data in the physiological range of membrane potentials. For example, we do not know how long it takes on average to open a Ca^{2+} channel at depolarizations that would be elicited by near threshold sounds. This lack of information currently also limits comparison of predictions resulting from realistic modelling of the biophysical properties of the hair cell synapse with descriptive models of cochlear coding of auditory threshold. Showing that the latency of the first spike in auditory neurons at all stages of the pathway can be uniformly described by a power function of the sound pressure envelope, Heil & Neubauer (2003) argued that the time and stimulus intensity dependence of auditory threshold is governed by a cochlear mechanism. Referring to the supralinear dependence of hair cell exocytosis on the intracellular $[Ca^{2+}]$ (Beutner *et al.* 2001) they suggested that hair cell synaptic coding could give rise to their power of four function for threshold. Considering the low Ca^{2+} cooperativity of exocytosis during depolarization in the physiological range of extracellular $[Ca^{2+}]$ (Brandt *et al.* 2005; Johnson *et al.* 2005; Keen & Hudspeth, 2006) it seems rather unlikely that exocytosis itself could account for their finding. At present it seems that auditory coding has to face significant signalling delays at the hair cell synapse, which are largely due to the time needed for Ca^{2+} channel gating. For the sake of temporal acuity in sound coding this temporal offset should be as constant as possible. One mechanism that potentially could contribute to achieve this, the parallel recruitment of several channel-release site units during brief depolarizations, is discussed in the next section.

A large readily releasable pool supports parallel release of several vesicles

Recordings of presynaptic capacitance changes and membrane fluorescence imaging showed that hair cells contain many readily releasable vesicles (Moser & Beutner, 2000; Edmonds *et al.* 2004; Spassova *et al.* 2004; Griesinger *et al.* 2005; Khimich *et al.* 2005; Schnee *et al.* 2005; Rutherford & Roberts, 2006). Converting capacitance or fluorescence changes into numbers of fused vesicles it was indicated that each ribbon-type active zone contains a readily releasable pool of tens of vesicles that can be released within a few milliseconds. This implied that the active zone should be capable of quasi 'simultaneously' releasing multiple vesicles achieving high rates of transmitter release. Highly synchronized release of multiple vesicles was demonstrated by recordings of excitatory postsynaptic currents from auditory nerve terminals (Glowatzki & Fuchs, 2002).

A reduction of the RRP was observed in mouse mutants for the presynaptic scaffolding protein Bassoon, whose IHCs mostly lack synaptic ribbons (Khimich *et al.* 2005). The time constant of pool depletion was unchanged, indicating that the release probability of the remaining readily releasable vesicles was not affected. From these findings it was concluded that the ribbon stabilizes a large readily releasable pool, potentially by concentrating docked vesicles at the active zone. Despite several readily releasable vesicles remained available at the mutant active zones the number of synchronously activated postsynaptic neurons, measured as amplitude of the compound action potential of the spiral ganglion, was greatly reduced in the Bassoon mutants. This indicated that the large RRP is important for temporally precise auditory coding at each hair cell synapse, probably because it enables parallel recruitment of channel-release site units. Hence, although a single vesicle may be sufficient to trigger a postsynaptic action potential (Siegel, 1992) temporally precise coding seems to require synchronous release of several vesicles. Postsynaptic detection of coincident release events could reduce the temporal variance introduced by pre- and postsynaptic mechanisms. Perhaps most importantly, such a design could neutralize temporal jitter imposed by the stochastic gating of the Ca^{2+} channels.

Combining a Ca^{2+} nanodomain control of exocytosis with a large number of channel-release site units and a large postsynaptic density containing many rapidly gating glutamate receptors (Glowatzki & Fuchs, 2002) the ribbon synapse of hair cells could achieve the temporal acuity required for auditory processing. The hair cell's synaptic design contrasts with that of large central auditory synapses, such as the endbulb and the calyx of Held (Fig. 3). For example, the calyx of Held holds hundreds of small active zones for reliable and temporally precise transmission onto a single (large) neuron (Fig. 3*B*, reviewed in von Gersdorff & Borst, 2002). This averaging over many active zones reduces the temporal jitter that would be imposed on synaptic transmission by stochastic Ca^{2+} channel opening and vesicle release if it relied on a single small active zone. However, at the first mammalian auditory synapse the whole task is placed onto an individual large active zone and its postsynaptic terminal (Fig. 3*A*).

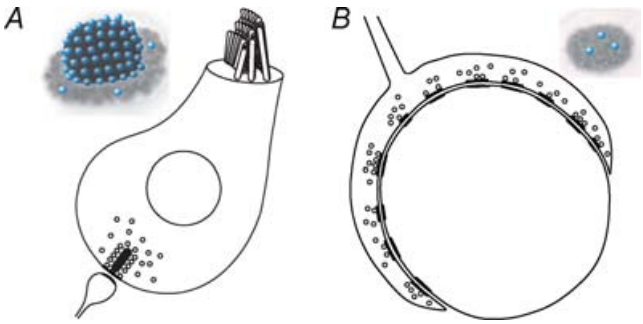

Figure 3. Two different designs for temporally precise synaptic transmission
A, schematic section of a IHC afferent synapse. The inset illustrates the IHC active zone with a synaptic ribbon (black), holding 16–30 synaptic vesicles (blue) docked to the presynaptic membrane (grey).
B, schematic section through a calyx of Held presynaptic terminal with many small active zones each holding only a few docked vesicles (see inset). For clarity non-docked vesicles have been removed from the inset.

Conclusions

Hair cells employ a whole set of mechanisms to achieve the extraordinary temporal acuity of sound coding with chemical synaptic transmission: short membrane time constants, Ca^{2+} nanodomain control of vesicle exocytosis, large readily releasable pool with parallel exocytosis of multiple vesicles and rapid gating of postsynaptic AMPA receptors. Due to the specific functional coupling of $Ca_V1.3$ channels and vesicle release sites the synapse probably makes limited use of the Ca^{2+}-dependent kinetics of exocytosis. Providing saturating $[Ca^{2+}]$ to the synaptic vesicle, it may exclusively build on the most rapid range of exocytosis kinetics. This minimizes the delay added by exocytosis and makes the activation of the Ca^{2+} channel the rate limiting step for synaptic transmission. Although this model is attractive, for it readily explains several aspects of sound coding, further experiments are needed to test it.

In particular, we will need to work out in more detail the molecular anatomy of the active zone. Electron tomography and immunoelectron microscopy of synapses from normal and genetically manipulated mice will help to explore the physical relationship between Ca^{2+} channels and synaptic vesicles and to reveal potential molecular links. High resolution light microscopy such as Stimulated Emission Depletion microscopy will advance our understanding of the active zone organization. To further address how high temporal fidelity of sound coding is achieved, future work should also investigate the near threshold behaviour of Ca^{2+} channel gating, the synaptic delay and the rate of transmitter release. The latter should preferentially be investigated by cell-attached measurements and paired pre- and postsynaptic recordings (Keen & Hudspeth, 2006). Because the number of paired pre- and postsynaptic recordings to be performed is limited by the substantial experimental effort, independent measurements of presynaptic and postsynaptic properties will continue to be of importance. The physiological analysis of mutants with defects in synaptic transmission will help us to understand hair cell synaptic function at the molecular, cellular and multicellular levels.

References

Augustine GJ (2001). How does calcium trigger neurotransmitter release? *Curr Opin Neurobiol* **11**, 320–326.

Augustine GJ, Adler EM & Charlton MP (1991). The calcium signal for transmitter secretion from presynaptic nerve terminals. *Ann N Y Acad Sci* **635**, 365–381.

Beutner D & Moser T (2001). The presynaptic function of mouse cochlear inner hair cells during development of hearing. *J Neurosci* **21**, 4593–4599.

Beutner D, Voets T, Neher E & Moser T (2001). Calcium dependence of exocytosis and endocytosis at the cochlear inner hair cell afferent synapse. *Neuron* **29**, 681–690.

Brandt A, Khimich D & Moser T (2005). Few CaV1.3 channels regulate the exocytosis of a synaptic vesicle at the hair cell ribbon synapse. *J Neurosci* **25**, 11577–11585.

Brandt A, Striessnig J & Moser T (2003). CaV1.3 channels are essential for development and presynaptic activity of cochlear inner hair cells. *J Neurosci* **23**, 10832–10840.

Dallos P (1985). Response characteristics of mammalian cochlear hair cells. *J Neurosci* **5**, 1591–1608.

Edmonds BW, Gregory FD & Schweizer FE (2004). Evidence that fast exocytosis can be predominantly mediated by vesicles not docked at active zones in frog saccular hair cells. *J Physiol* **560**, 439–450.

Fuchs PA (2005). Time and intensity coding at the hair cell's ribbon synapse. *J Physiol* **566**, 7–12.

Furukawa T, Hayashida Y & Matsuura S (1978). Quantal analysis of the size of excitatory post-synaptic potentials at synapses between hair cells and afferent nerve fibres in goldfish. *J Physiol* **276**, 211–226.

Furukawa T, Kuno M & Matsuura S (1982). Quantal analysis of a decremental response at hair cell-afferent fibre synapses in the goldfish sacculus. *J Physiol* **322**, 181–195.

Furukawa T & Matsuura S (1978). Adaptive rundown of excitatory post-synaptic potentials at synapses between hair cells and eight nerve fibres in the goldfish. *J Physiol* **276**, 193–209.

Glowatzki E & Fuchs PA (2002). Transmitter release at the hair cell ribbon synapse. *Nat Neurosci* **5**, 147–154.

Griesinger CB, Richards CD & Ashmore JF (2005). Fast vesicle replenishment allows indefatigable signalling at the first auditory synapse. *Nature* **435**, 212–215.

Grothe B (2003). New roles for synaptic inhibition in sound localization. *Nat Rev Neurosci* **4**, 540–550.

Grothe B & Klump GM (2000). Temporal processing in sensory systems. *Curr Opin Neurobiol* **10**, 467–473.

Heil P & Neubauer H (2003). A unifying basis of auditory thresholds based on temporal summation. *Proc Natl Acad Sci U S A* **100**, 6151–6156.

Hess P, Lansman JB & Tsien RW (1984). Different modes of Ca channel gating behaviour favoured by dihydropyridine Ca agonists and antagonists. *Nature* **311**, 538–544.

Issa NP & Hudspeth AJ (1994). Clustering of Ca^{2+} channels and Ca^{2+}-activated K^+ channels at fluorescently labeled presynaptic active zones of hair cells. *Proc Natl Acad Sci U S A* **91**, 7578–7582.

Johnson DH (1980). The relationship between spike rate and synchrony in responses of auditory-nerve fibers to single tones. *J Acoust Soc Am* **68**, 1115–1122.

Johnson SL, Marcotti W & Kros CJ (2005). Increase in efficiency and reduction in Ca^{2+} dependence of exocytosis during development of mouse inner hair cells. *J Physiol* **563**, 177–191.

Keen EC & Hudspeth AJ (2006). Transfer characteristics of the hair cell's afferent synapse. *Proc Natl Acad Sci U S A* **103**, 5537–5542.

Kennedy HJ, Evans MG, Crawford AC & Fettiplace R (2003). Fast adaptation of mechanoelectrical transducer channels in mammalian cochlear hair cells. *Nat Neurosci* **6**, 832–836.

Kharkovets T, Dedek K, Maier H, Schweizer M, Khimich D, Nouvian R, Vardanyan V, Leuwer R, Moser T & Jentsch TJ (2006). Mice with altered KCNQ4 K^+ channels implicate sensory outer hair cells in human progressive deafness. *EMBO J* **25**, 642–652.

Khimich D, Nouvian R, Pujol R, Tom Dieck S, Egner A, Gundelfinger ED & Moser T (2005). Hair cell synaptic ribbons are essential for synchronous auditory signalling. *Nature* **434**, 889–894.

Kiang NY-S, Watanabe T, Thomas EC & Clark LF (1965). *Discharge Pattern of Single Fibers in the Cat's Auditory Nerve*. MIT Press, Cambridge, MA, USA.

Konishi M (2003). Coding of auditory space. *Annu Rev Neurosci* **26**, 31–55.

Koschak A, Reimer D, Huber I, Grabner M, Glossmann H, Engel J & Striessnig J (2001). α1D (Cav1.3) subunits can form L-type Ca^{2+} channels activating at negative voltages. *J Biol Chem* **276**, 22100–22106.

Kros CJ & Crawford AC (1990). Potassium currents in inner hair cells isolated from the guinea-pig cochlea. *J Physiol* **421**, 263–291.

Kros CJ, Ruppersberg JP & Rusch A (1998). Expression of a potassium current in inner hair cells during development of hearing in mice. *Nature* **394**, 281–284.

McAlpine D (2005). Creating a sense of auditory space. *J Physiol* **566**, 21–28.

McAlpine D & Grothe B (2003). Sound localization and delay lines – do mammals fit the model? *Trends Neurosci* **26**, 347–350.

Marcotti W, Johnson SL, Holley MC & Kros CJ (2003). Developmental changes in the expression of potassium currents of embryonic, neonatal and mature mouse inner hair cells. *J Physiol* **548**, 383–400.

Matsubara A, Laake JH, Davanger S, Usami S & Ottersen OP (1996). Organization of AMPA receptor subunits at a glutamate synapse: a quantitative immunogold analysis of hair cell synapses in the rat organ of Corti. *J Neurosci* **16**, 4457–4467.

Michna M, Knirsch M, Hoda JC, Muenkner S, Langer P, Platzer J, Striessnig J & Engel J (2003). Cav1.3 (α1D) Ca^{2+} currents in neonatal outer hair cells of mice. *J Physiol* **553**, 747–758.

Mintz IM, Sabatini BL & Regehr WG (1995). Calcium control of transmitter release at a cerebellar synapse. *Neuron* **15**, 675–688.

Moser T & Beutner D (2000). Kinetics of exocytosis and endocytosis at the cochlear inner hair cell afferent synapse of the mouse. *Proc Natl Acad Sci U S A* **97**, 883–888.

Nouvian R, Beutner D, Parsons TD & Moser T (2006). Structure and function of the hair cell ribbon synapse. *J Membr Biol* **209**, 153–165.

Oliver D, Knipper M, Derst C & Fakler B (2003). Resting potential and submembrane calcium concentration of inner hair cells in the isolated mouse cochlea are set by KCNQ-type potassium channels. *J Neurosci* **23**, 2141–2149.

Oliver D, Taberner AM, Thurm H, Sausbier M, Arntz C, Ruth P, Fakler B & Liberman MC (2006). The role of BKCa channels in electrical signal encoding in the mammalian auditory periphery. *J Neurosci* **26**, 6181–6189.

Palmer AR & Russell IJ (1986). Phase-locking in the cochlear nerve of the guinea-pig and its relation to the receptor potential of inner hair-cells. *Hear Res* **24**, 1–15.

Platzer J, Engel J, Schrott-Fischer A, Stephan K, Bova S, Chen H, Zheng H & Striessnig J (2000). Congenital deafness and sinoatrial node dysfunction in mice lacking class D L-type Ca^{2+} channels. *Cell* **102**, 89–97.

Ricci AJ, Kennedy HJ, Crawford AC & Fettiplace R (2005). The transduction channel filter in auditory hair cells. *J Neurosci* **25**, 7831–7839.

Roberts WM, Jacobs RA & Hudspeth AJ (1990). Colocalization of ion channels involved in frequency selectivity and synaptic transmission at presynaptic active zones of hair cells. *J Neurosci* **10**, 3664–3684.

Robertson D & Paki B (2002). Role of L-type Ca^{2+} channels in transmitter release from mammalian inner hair cells. II. Single-neuron activity. *J Neurophysiol* **87**, 2734–2740.

Rodriguez-Contreras A & Yamoah EN (2001). Direct measurement of single-channel Ca^{2+} currents in bullfrog hair cells reveals two distinct channel subtypes. *J Physiol* **534**, 669–689.

Rodriguez-Contreras A & Yamoah EN (2003). Effects of permeant ion concentrations on the gating of L-type Ca^{2+} channels in hair cells. *Biophys J* **84**, 3457–3469.

Rose JE, Brugge JF, Anderson DJ & Hind JE (1967). Phase-locked response to low-frequency tones in single auditory nerve fibers of the squirrel monkey. *J Neurophysiol* **30**, 769–793.

Rutherford MA & Roberts WM (2006). Frequency selectivity of synaptic exocytosis in frog saccular hair cells. *Proc Natl Acad Sci U S A* **103**, 2898–2903.

Schnee ME, Lawton DM, Furness DN, Benke TA & Ricci AJ (2005). Auditory hair cell-afferent fiber synapses are specialized to operate at their best frequencies. *Neuron* **47**, 243–254.

Schnee ME & Ricci AJ (2003). Biophysical and pharmacological characterization of voltage-gated calcium currents in turtle auditory hair cells. *J Physiol* **549**, 697–717.

Sewell WF (1984). The relation between the endocochlear potential and spontaneous activity in auditory nerve fibres of the cat. *J Physiol* **347**, 685–696.

Sidi S, Busch-Nentwich E, Friedrich R, Schoenberger U & Nicolson T (2004). *gemini* encodes a zebrafish L-type calcium channel that localizes at sensory hair cell ribbon synapses. *J Neurosci* **24**, 4213–4223.

Siegel JH (1992). Spontaneous synaptic potentials from afferent terminals in the guinea pig cochlea. *Hear Res* **59**, 85–92.

Spassova MA, Avissar M, Furman AC, Crumling MA, Saunders JC & Parsons TD (2004). Evidence that rapid vesicle replenishment of the synaptic ribbon mediates recovery from short-term adaptation at the hair cell afferent synapse. *J Assoc Res Otolaryngol* **5**, 376–390.

Spassova M, Eisen MD, Saunders JC & Parsons TD (2001). Chick cochlear hair cell exocytosis mediated by dihydropyridine-sensitive calcium channels. *J Physiol* **535**, 689–696.

Thurm H, Fakler B & Oliver D (2005). Ca^{2+}-independent activation of BKCa channels at negative potentials in mammalian inner hair cells. *J Physiol* **569**, 137–151.

Tucker T & Fettiplace R (1995). Confocal imaging of calcium microdomains and calcium extrusion in turtle hair cells. *Neuron* **15**, 1323–1335.

von Gersdorff H & Borst JG (2002). Short-term plasticity at the calyx of Held. *Nat Rev Neurosci* **3**, 53–64.

Wu LG, Westenbroek RE, Borst JG, Catterall WA & Sakmann B (1999). Calcium channel types with distinct presynaptic localization couple differentially to transmitter release in single calyx-type synapses. *J Neurosci* **19**, 726–736.

Zenisek D, Davila V, Wan L & Almers W (2003). Imaging calcium entry sites and ribbon structures in two presynaptic cells. *J Neurosci* **23**, 2538–2548.

Zhang SY, Robertson D, Yates G & Everett A (1999). Role of L-type Ca^{2+} channels in transmitter release from mammalian inner hair cells I. Gross sound-evoked potentials. *J Neurophysiol* **82**, 3307–3315.

Zidanic M & Fuchs PA (1995). Kinetic analysis of barium currents in chick cochlear hair cells. *Biophys J* **68**, 1323–1336.

Zucker RS & Fogelson AL (1986). Relationship between transmitter release and presynaptic calcium influx when calcium enters through discrete channels. *Proc Natl Acad Sci U S A* **83**, 3032–3036.

Acknowledgements

Work was supported by grants of the DFG (SFB406 and CMPB), the European Commission (through the integrated project EuroHear), the Human Frontiers Science Program (HFSP) and the federal goverment (through the Bernstein Center for Computational Neuroscience, Göttingen) to T. Moser. We would like to thank Michael Avissar and Thomas D. Parsons for providing single unit data (Fig. 1*B*) and Michael Avissar, Thomas D. Parsons, W. Roberts, M. Rutherford and Fred Wolf for feedback on the MS.